Experimental and Analytical Studies of a Horizontally Curved Steel I-Girder Bridge during Erection

D. Linzell[1]; R. T. Leon[2]; and A. H. Zureick[3]

Abstract: A series of studies on an experimental, full-scale curved steel bridge structure during erection are discussed. The work was part of the Federal Highway Administration's curved steel bridge research project (CSBRP). The CSBRP is intended to improve the understanding of curved bridge behavior and to develop more rational design guidelines. The main purpose of the studies reported herein was to assess the capability of analytical tools for predicting response during erection. Nine erection studies, examining six different framing plans, are presented. The framing plans are not necessarily representative of curved bridge subassemblies as they would be erected in the field; however, they represent a variety of conditions that would test the robustness of analysis tools and assess the importance of erection sequence on initial stresses in a curved girder bridge. The simply supported, three I-girder system used for the tests is described and methods for reducing and examining the data are discussed. Comparisons between experimental and analytical results demonstrate that analysis tools can predict loads and deformations during construction. Comparison to the V-load method indicates that it predicts stresses in exterior girders well, but can underpredict them for interior girders.

DOI: 10.1061/(ASCE)1084-0702(2004)9:6(521)

CE Database subject headings: Bridges, girder; Bridges, steel; Bridge construction; Curvature; Experimentation.

Introduction

The use of curved steel bridges in the United States has increased dramatically over the past 25 years, to where they constitute nearly one-third of all bridges being built today. Curved steel bridges are often the only structures that can be accommodated within the limited space available in urban traffic corridors while maintaining required design speeds. In addition, curved steel bridges often result in an aesthetically superior solution. However, the lack of guidelines for construction, the perceived overconservatism of certain aspects of the American Association of State Highway and Transportation Officials (AASHTO) *Guide specifications for horizontally curved bridges* (AASHTO 1980, 1993, 2003) and the need for bridges of tighter radii indicate that further research is required to refine the available design recommendations.

Based on a long-range plan prepared by American Institute of Steel Construction (AISC) Marketing, Inc. (AISC 1989), a synthesis of research needs for curved steel bridges (Yadlosky 1991), which highlighted some of the aforementioned limitations, increased awareness of the need to reexamine how curved steel bridges behave. In 1992, the curved steel bridge research project (CSBRP) was initiated by the Federal Highway Administration (FHwA). The project has multiple tasks, ranging from review of the existing research (Zureick et al. 1994; Zureick and Naqib 1999) to development of new design provisions. The centerpiece of the project is the testing of large-scale curved bridge girder sections under realistic boundary conditions. The tests were designed to examine the performance of various curved I-girder cross sections under bending, shear, and combined bending and shear behavior. Large-scale testing was deemed essential to develop more realistic design provisions, because experimental work performed for the original AASHTO Guide Specifications involved only 1/20-scale to 1/2-scale component and model tests under artificial boundary conditions.

Prior to the bending tests, a series of initial studies were completed during erection of the experimental curved bridge structure. These tests provided a unique opportunity to study the erection behavior of a large-scale curved steel bridge in a laboratory environment. Behavior of curved girder bridges can be sensitive to construction sequence due to the girders' natural tendency to twist and warp during erection, when members behave as individual units rather than a complete three-dimensional structural system. This can lead to unexpected global and local deformations after construction and under service loads. This paper describes the structure tested for the erection studies and bending component tests, summarizes instrumentation used for the erection studies, and discusses the erection tests and their results.

Background

Understanding and quantifying curved beam behavior has been the focus of numerous investigations. The behavior of curved steel bridges did not become a major research focus until the 1960s, when the advantages of curved steel bridges were recognized and the need to develop a design specification arose. De-

[1]Assistant Professor, Dept. of Civil and Environmental Engineering, The Pennsylvania State Univ., University Park, PA 16802.

[2]Professor, School of Civil and Environmental Engineering, Georgia Tech, Atlanta, GA 30332-0355.

[3]Professor, School of Civil and Environmental Engineering, Georgia Tech, Atlanta, GA 30332–0355.

Note. Discussion open until April 1, 2005. Separate discussions must be submitted for individual papers. To extend the closing date by one month, a written request must be filed with the ASCE Managing Editor. The manuscript for this paper was submitted for review and possible publication on May 4, 2000; approved on September 23, 2003. This paper is part of the ***Journal of Bridge Engineering***, Vol. 9, No. 6, November 1, 2004. ©ASCE, ISSN 1084-0702/2004/6-521–530/$18.00.

velopment of these specifications in the United States began with the Consortium of University Research Teams (CURT) project in the late 1960s and continued until the mid-1970s, culminating with publication of the first AASHTO *Guide specifications for horizontally curved bridges* (1980). Significant research on curved girders was also carried out in Japan, beginning in the late 1970s and extending into the early 1980s, as part of development of the Hanshin Expressway Public Corporation's (1988) *Guidelines for the Design of Horizontally Curved Girder Bridges*. A summary of Japanese curved bridge experimental plate and box-girder research completed for the Hanshin guidelines was provided by Kitada et al. (1993).

Detailed summaries and critiques of the most significant curved girder research can be found in Zureick et al. (1994), Zureick and Naqib (1999), Linzell (1999), and Hall et al. (1999). Details of those summaries will not be repeated here, but information gathered for those studies was used in the initial phases of the CSBRP to identify significant shortcomings associated with existing experimental data. The first significant shortcoming is that the experimental studies carried out by CURT and others included only small-scale tests of model bridges and of medium-scale models of individual components under idealized loading and boundary conditions. Brennan (1970, 1971), for example, performed an extensive set of studies on $\frac{1}{6.67}$ scale models of two continuous curved I-girder spans for the Seekonk River Bridge, and Mozer and Culver (1970) and Mozer et al. (1971, 1973) tested individual girders and girder pairs. Full-scale tests of large curved girders or complete structures at large scales have not been carried out. The second shortcoming is that most of the tests examined the behavior of noncomposite systems under static loads, although some work on composite curved steel-concrete bridge systems (Colville 1973) and on systems under dynamic loads (Armstrong 1972) was conducted. Since the CURT project, several other notable model tests of single curved I-girders (Yoo and Carbine 1985; Shanmugam et al. 1995; Thevendran et al. 1998) have been carried out, but the two shortcomings noted previously still remain. Finally, the aforementioned studies did not explicitly examine the behavior of curved steel bridges during erection, although work completed for the CURT project did examine curved bridge behavior before and after a deck was placed (Brennan 1970). Recently, a field study was carried out that examined the erection behavior of a two-span continuous horizontally curved and superelevated I-girder structure (Galambos et al. 1996). The superstructure was instrumented with strain gauges and readings were taken after placement of all or a portion of the spans and prior to and after tightening the bolted connections. Data were also recorded during placement of the deck and long-term measurements were made. Recorded strains in the girders and cross frames were compared to analysis values as presented by Huang (1996). Findings from the studies indicated that

- Stiffness controlled behavior during the erection stages in which the structure was shored;
- Computed girder deflections and strains matched well with experimental values for the analyses, with differences that existed being attributed to erratic warping restraint conditions that occurred;
- Stresses in the cross frames during fitup of the structure were low and were difficult to predict accurately; and
- A minimum of 958–1,437 Pa (20–30 psf) of live load needed to be included in the models to accurately represent maximum construction stresses.

Because of the limited information available on construction behavior of horizontally curved steel bridges, it is intended to present information related to the accuracy with which analytical tools predicted the response of the CSBRP experimental curved bridge structure during erection. Two limitations of this work should be clearly understood. First, while the erection studies discussed herein do provide valuable information related to load redistribution during construction, they should not be construed as realistically simulating the erection sequence for any particular bridge. Second, the primary intent of the CSBRP was to provide a set of benchmark data that could test the robustness of available analytical tools for predicting the behavior of large curved girders under realistic boundary conditions. The structure used for the studies, however, should not be construed as a prototype of a realistic bridge.

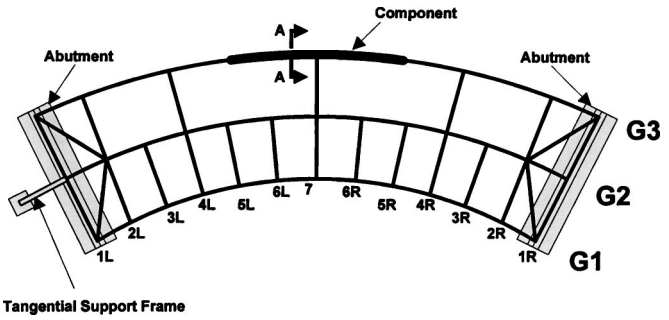

Fig. 1. Framing plan

Experimental Plan

As noted earlier, the centerpiece of the CSBRP was the testing of large-scale curved I-girder sections under realistic loading and boundary conditions. After a number of feasibility and analytical studies, a simply supported three-girder system with a median span of 27.4 m (90 ft 0 in.) was selected as the testing frame. A framing plan schematic is shown in Fig. 1 and a photograph is given in Fig. 2. From preliminary analytical studies, the three-girder system was considered sufficient to estimate the complex load distribution patterns that can arise in these structures. In addition, the tight girder radii that were used permitted testing girder geometries under similar conditions to those encountered in practice today.

Girder spans ranged between 26.2 and 28.6 m (8 ft 0 in. and 93 ft 11 in.) along the arc, with radii of curvature between 58.3 and 63.6 m (191 ft 3 in. and 208 ft 0 in.). Girder plate dimensions are summarized in Table 1. All of the girders were cambered vertically. Recambering was required for G2 because during initial fabrication the girder was incorrectly cambered after all of its stiffeners and bearing plates had been attached. Recambering was accomplished through a series of "V" heats of segments of the girder web, with the base of each "V" located near the bottom flange.

So that the experimental curved bridge could be used for a number of studies, it was required that a large portion of the system remained elastic. This not only dictated girder, cross-frame, and lower lateral bracing dimensions, but it also forced an increase in steel strength for G2 from ASTM A 572 Grade 50 to AASHTO M270 Grade 70 W. Another byproduct of the desire to maintain elastic behavior was the cross-frame placement scheme shown in Fig. 1. Extra lines of cross frames were placed between G1 and G2 to stiffen and stabilize the inner girder pair. In addi-

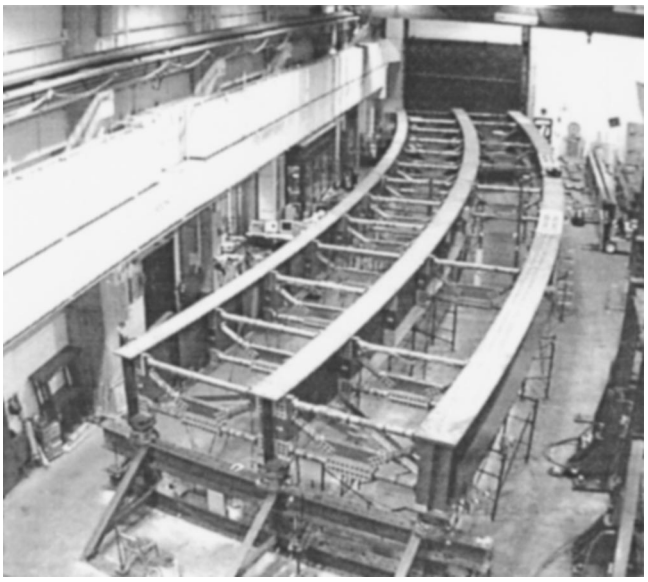

Fig. 2. Experimental curved bridge

tion, cross frames were constructed of five high strength steel tubular members (413 MPa, 60 ksi) arranged in a K-type frame. This design minimized the possibility of yielding and simplified instrumentation of individual cross-frame members so that their forces could be monitored.

Instrumentation

Extensive instrumentation was used to monitor behavior during erection. Load cells were placed at girder abutment supports and at intermediate shoring locations. Strain gauges were placed onto the girders (Fig. 3), cross frames, and lower lateral bracing. Resistance gauges were used for the cross frames and bracing members, while vibrating wire gauges were placed onto the girders.

Girder deformations were measured at midspan and the abutments using standard displacement and rotation transducers (potentiometers, linear variable differential transducers, and tiltmeters; Fig. 4) and at set increments along the top and/or bottom flanges of each girder using laser and total station systems. The transducers provided detailed deformation data at the selected bridge cross sections while the laser and total station systems provided global deformations.

The quantity of instruments acquired for each erection study test was directly related to the number of structural components that were installed. Therefore, instrument quantities increased with each test, with the first test acquiring approximately 70 individual data points while the final test acquired approximately 1,050 data points.

Table 1. Girder Plate Dimensions

Location	Flanges $b_f \times t_f$ [mm (in.)]	Web $h_w \times t_w$ [mm (in.)]
G1	$406 \times 27\ (16 \times 1\ \frac{1}{16})$	$1{,}219 \times 11\ (48 \times \frac{7}{16})$
G2	$508 \times 30\ (20 \times 1\ \frac{3}{16})$	$1{,}219 \times 13\ (48 \times \frac{1}{2})$
G3	$610 \times 57\ (24 \times 2\ \frac{1}{4})$	$1{,}219 \times 13\ (48 \times \frac{1}{2})$

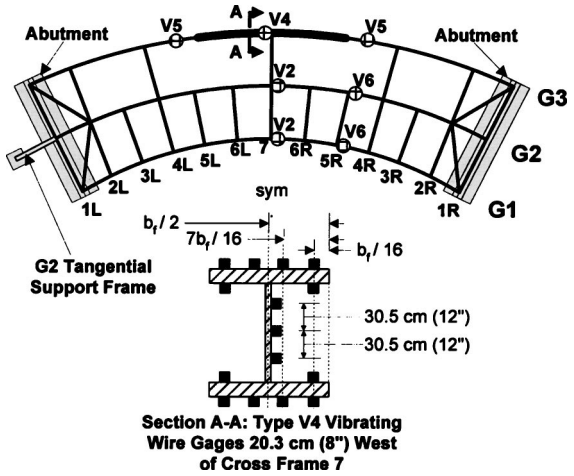

Fig. 3. Girder strain gauge locations

Erection Study Tests

Prior to each erection study test, the structure was shored so that strains due to its self-weight would be minimized. This was accomplished by recreating the prescribed design camber in the laboratory. Girder midspan camber elevations were set as close as possible to measurements taken during preassembly of the structure at the fabrication shop. Then, abutment and shoring load cell readings were adjusted until they matched well with the support reactions predicted using preliminary analyses. Once acceptable loads cell readings had been established, the system was said to be in a "no-load" condition and testing began. Single intermediate shores or groups of shores were sequentially removed until the system was fully deflected under its own self-weight. Shoring was then sequentially reinstalled until the system returned to the "no-load" condition. At this point, the test was terminated. Data was recorded after each removal and replacement step. Those tests in which shoring was removed from beneath only the interior girder (G1) in a twin-girder system were termed ES1 studies. Those that removed shoring from beneath both girders (G1 and G2) in a twin-girder system were termed ES2 studies. Finally, the single test in which intermediate supports were removed from beneath the three-girder system was called ES3-1. Framing plans for the

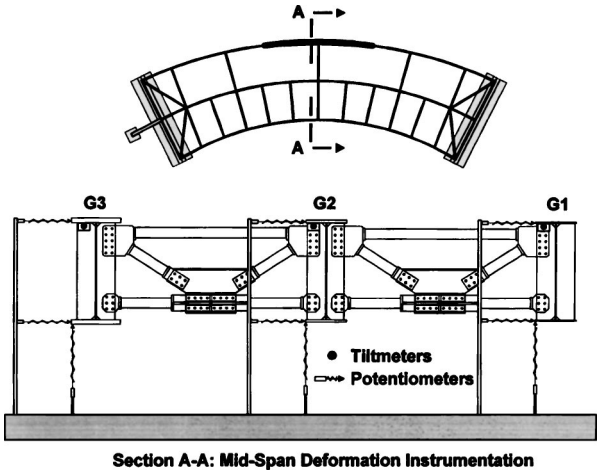

Fig. 4. Girder midspan deformation instruments

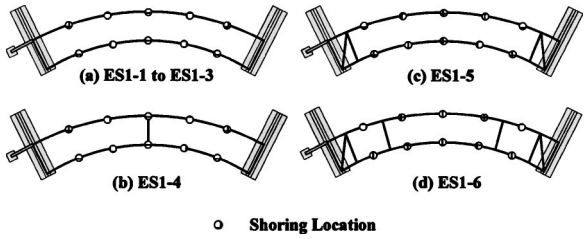

Fig. 5. Erection study framing plans, ES1 series: (a) ES1-1 to ES1-3; (b) ES1-4; (c) ES1-5; and (d) ES1-6

ES1, ES2, and ES3 tests are shown in Figs. 5–7. The circles in these figures indicate the location of intermediate shoring frames, each of which contained a load cell (300 kip capacity at the abutment supports and 100 kip capacity at the shoring frames). Data from an individual load cell location was labeled relative to the girder and cross-frame number as shown in Fig. 1 (i.e., G1-1L refers to a reading at left cross frame number 1 where it intersects G1).

Single-Girder Studies (ES1)

Six single-girder erection tests were performed to examine the response of girder G1 under different lateral support conditions. For the first three tests, ES1-1 through ES1-3 as shown in Fig. 5, both girders G1 and G2 were connected using end cross frames 1L and 1R only, with shoring initially provided at five locations beneath each girder as shown in Fig. 5(a). With G2 being shored throughout the entire duration of each ES1 test, shoring beneath girder G1 was removed beginning with the shoring located at cross frames 3L, 5L, 3R, and 5R, which left the girder supported at the midspan shoring location (location 7 in Fig. 1). This support was then used to lower G1 to its final deflected state. Reactions at each vertical support both before and after the removal of G1 shoring are shown for all the ES1 tests in Table 2.

The two initial single-girder tests, ES1-1 and ES1-2, were brief trials intended to examine the performance of the data acquisition systems as G1 was allowed to deflect elastically. At the completion of the lowering portion of these tests, G1 midspan vertical displacement (Fig. 4) was 146 mm $\left(5\frac{3}{4}\text{ in.}\right)$ for ES1-1 and 171 mm $\left(6\frac{3}{4}\text{ in.}\right)$ for ES1-2, with each test being terminated before G1 reached its predicted maximum midspan vertical displacement. For ES1-3, the first test for which explicit shoring removal and replacement schemes were followed and the first for which G1 was permitted to reach its anticipated full elastic deflection, G1 midspan vertical displacement (Fig. 4) was 254 mm (10 in.) accompanied by 13° of radial rotation. This extreme case of an unshored curved I-girder with a large unbraced length clearly illustrated the large elastic flexibility of curved girders.

To examine the response of girder G1 in the presence of one additional intermediate cross frame, test ES1-4 was conducted. In this case, a cross frame at midspan between the girders (location 7 in Fig. 1) was added while both girders G1 and G2 were shored. After removing shoring beneath girder G1, its midspan vertical deflection (Fig. 4) was 8 mm (0.3 in.), accompanied by a minimal rotation (less than 0.1°). This represents a reduction of almost two orders of magnitude (32 times for deflection and 130 times for rotation) as compared to the case with no bracing at midspan. Reactions at the beginning and end of ES1-4 are shown in Table 2. This case clearly illustrated the critical role that midspan lateral restraint plays during the erection of curved steel girders. For ES1-5, cross frames 1L and 1R, adjacent to frames 2L and 2R, and lower lateral bracing in the outer bays were provided with girders G1 and G2 being shored, as shown in Fig. 5(c). Upon removal of shoring beneath G1, the midspan displacement of girder G1 (Fig. 4) was 46 mm (1.8 in.), accompanied by 0.65° radial rotation. For ES1-6 [Fig. 5(d)], cross frames 4L and 4R were added to those already in place at the completion of ES1-5. The vertical displacement of G1 was 11 mm (0.45 in.), about one-fourth of that of test ES1-5. G1 rotation for this case was 1.25°.

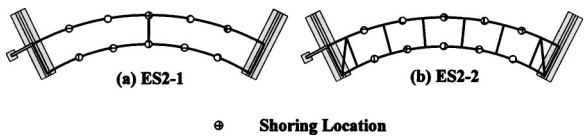

Fig. 6. Erection study framing plans, ES2 series: (a) ES2-1; and (b) ES2-2

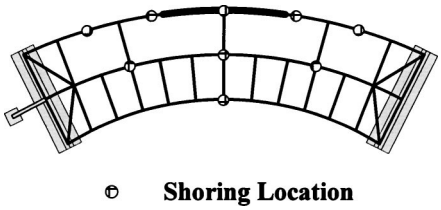

Fig. 7. Erection study framing plan, ES3-1

Two-Girder Studies (ES2)

For the twin-girder behavior, two tests were completed (Fig. 6). Test ES2-1 took place immediately after completion of ES1-4 and studied the same framing plan but lowered both G1 and G2 to their final deflected shapes. Measured midspan displacements (Fig. 4) were 18 mm (0.7 in.) for G1 and 63 mm (2.5 in.) for G2. The accompanying radial rotations at midspan were 1° for G1 and G2. Test ES2-2 was completed with the lower lateral bracing and cross frames 1L, 2L, 4L, 6L, 6R, 4R, 2R, and 1R in-place. Maximum midspan displacements (Fig. 4) were 10 mm (0.4 in.) for G1 and 36 mm (1.4 in.) for G2 and were accompanied by midspan radial rotations of 0.5°.

Three-Girder Study (ES3-1)

A single test (ES3-1) was conducted to examine the behavior of the three-girder system as shoring was removed and replaced. Thirteen cross frames were placed between G1 and G2 and seven between G2 and G3 (Fig. 7). After the shoring was removed, midspan displacements and rotations (Fig. 4) were 5 mm (0.2 in.) and 0.2° for G1, 15 mm (0.6 in.) and 0.2° for G2, and 25 mm (1.0 in.) and 0.3° for G3. ES3-1 involved a series of additional investigations of each girder using a single midspan shore. Each girder was raised in lifts corresponding to equal load increments until its midspan shore reached 62.3 kN (14 kips) of load. Identical increments were then used to lower each girder back to its unshored state.

Although the test conditions were not intended to reproduce actual construction conditions, valuable insights were obtained for cases in which falsework, temporary shoring, or interior bents are used to stabilize a curved girder bridge during construction. It

Table 2. Abutment/Intermediate Shoring Frame Support Reaction Magnitudes, Shored and Unshored, ES1 Tests

			Support reaction at shoring location [kips (kN)]						
Test	Girder	Support condition	1L	3L	5L	7	5R	3R	1R
ES1-1	G1	Shored	2.0 (8.8)	2.1 (9.2)	2.0 (9.0)	2.1 (9.3)	2.1 (9.2)	2.4 (10.6)	2.6 (11.5)
		Unshored	4.7 (21.1)	0.0 (0.0)	0.0 (0.0)	7.8 (34.9)	0.0 (0.0)	0.0 (0.0)	5.3 (23.7)
	G2	Shored	—	—	—	—	—	—	—
		Unshored	—	—	—	—	—	—	—
ES1-2	G1	Shored	3.8 (17.1)	0.0 (0.0)	0.0 (0.0)	11.5 (51.0)	0.0 (0.0)	0.0 (0.0)	4.1 (18.2)
		Unshored	5.2 (23.2)	0.0 (0.0)	0.0 (0.0)	6.6 (29.2)	0.0 (0.0)	0.0 (0.0)	5.4 (24.0)
	G2	Shored	1.8 (7.9)	6.2 (13.6)	3.1 (13.6)	5.7 (25.5)	3.4 (15.1)	5.4 (23.9)	3.1 (13.6)
		Unshored	1.9 (8.4)	7.1 (31.4)	3.2 (14.4)	5.6 (24.9)	3.6 (16.1)	6.3 (28.2)	3.1 (13.8)
ES1-3	G1	Shored	3.9 (17.1)	0.0 (0.0)	0.0 (0.0)	11.6 (51.5)	0.0 (0.0)	0.0 (0.0)	4.1 (18.4)
		Unshored	6.1 (30.0)	0.0 (0.0)	0.0 (0.0)	4.0 (17.8)	0.0 (0.0)	0.0 (0.0)	6.2 (27.5)
	G2	Shored	1.9 (8.3)	6.2 (27.6)	3.1 (13.6)	5.7 (25.4)	3.4 (15.2)	5.4 (24.0)	3.0 (13.5)
		Unshored	2.0 (9.0)	7.5 (33.3)	3.3 (14.8)	5.5 (24.7)	3.7 (16.7)	6.8 (30.3)	3.3 (14.8)
ES1-4	G1	Shored	4.3 (19.3)	0.0 (0.0)	0.0 (0.0)	12.3 (54.8)	0.0 (0.0)	0.0 (0.0)	4.9 (21.8)
		Unshored	7.5 (33.5)	0.0 (0.0)	0.0 (0.0)	0.0 (0.0)	0.0 (0.0)	0.0 (0.0)	8.0 (35.7)
	G2	Shored	1.2 (5.2)	4.1 (18.1)	5.7 (25.5)	7.2 (32.1)	4.6 (20.6)	3.5 (15.4)	1.8 (8.1)
		Unshored	2.4 (10.6)	5.5 (24.5)	5.8 (25.9)	7.0 (31.0)	4.8 (21.5)	4.9 (21.8)	3.3 (14.7)
ES1-5	G1	Shored	1.9 (8.4)	3.8 (17.0)	2.1 (9.5)	4.4 (19.7)	2.2 (9.8)	1.4 (6.3)	4.3 (19.3)
		Unshored	7.4 (33.3)	0.0 (0.0)	0.0 (0.0)	0.0 (0.0)	0.0 (0.0)	0.0 (0.0)	8.4 (37.1)
	G2	Shored	3.6 (15.9)	4.9 (21.9)	3.8 (17.0)	5.0 (22.3)	5.1 (22.9)	4.6 (20.5)	3.0 (13.2)
		Unshored	5.6 (25.1)	3.2 (4.7)	4.6 (20.5)	8.1 (36.1)	4.9 (21.6)	4.1 (18.1)	4.6 (20.5)
ES1-6	G1	Shored	1.9 (8.3)	4.5 (20.0)	3.4 (15.2)	2.5 (11.3)	3.6 (16.2)	4.4 (19.6)	3.2 (14.3)
		Unshored	7.8 (34.7)	0.0 (0.0)	0.0 (0.0)	0.0 (0.0)	0.0 (0.0)	0.0 (0.0)	9.1 (40.7)
	G2	Shored	3.1 (13.7)	5.3 (23.8)	5.2 (23.2)	5.0 (22.4)	5.3 (23.7)	5.2 (23.1)	1.6 (7.2)
		Unshored	5.2 (23.2)	5.0 (22.1)	5.6 (24.7)	6.4 (28.3)	5.8 (26.0)	5.3 (23.7)	3.7 (16.3)

was demonstrated that it is desirable to unload the shoring uniformly to minimize unwanted twisting of the steel. However, uniform unloading is often difficult to achieve in the field. Procedures followed for the ES1 and ES2 studies provided data on the level of deformations and load redistribution that would result from nonuniform removal of temporary shoring supports. Once the intermediate shores were removed, the ES2 studies also provided information on the behavior of unshored paired girder systems, which are often erected in the field when site conditions prevent the use of extensive intermediate shoring.

Equilibrium Evaluations

Data reduction for the erection studies centered on a number of equilibrium checks that were meant to provide data for the erection studies and to verify the robustness and accuracy for predicting force distributions in the bridge. It was understood that both the construction sequence and material and geometric imperfections introduced during fabrication would impact the calculations. However, while these conditions can be accounted for in analytical models, oftentimes it is not practical for practitioners to include them. As an example, consider the effect of the recambering of G2. Reestablishing the correct camber made transverse stiffeners out-of-plumb, which resulted in fitup problems for the cross frames during erection. While for the tests described herein, these construction stresses could not be properly quantified, as all the necessary instrumentation was not in place when the affected cross frames were erected, even if measurements of the induced stresses during fitup were recorded, accurately replicating their effects in an analytical model would be difficult and would greatly increase solution time.

Overall external equilibrium calculations for the erection studies showed satisfactory results. Results were typically conservative and provided agreement within 5% for the summation of vertical forces and 10% for the summation of moments about the short dimension (width) of the bridge. Summation of horizontal forces and resulting moments for both the radial and tangential directions gave slightly larger differences (10–25%). This was expected as the horizontal reactions at the supports were generally small when compared with the vertical reactions (10% or less) and were not precisely quantified because of the influence of friction on bearing behavior. Maximum differences for internal equilibrium calculations were nearly 30% for moments about the radial and tangential directions and resulted primarily from conditions where the horizontal reactions at the supports unduly influenced the results for equilibrium of one-half of the structure. When the equilibium of one-half of the structure was taken about midspan, the moment arms ($\approx$14 m or 45 ft) of the radial forces at the bearings had a disproportionate effect on equilibrium calculations.

Analytical Comparisons

A finite-element model, containing over 8,400 elements and 50,000 degrees of freedom, was assembled using ABAQUS to

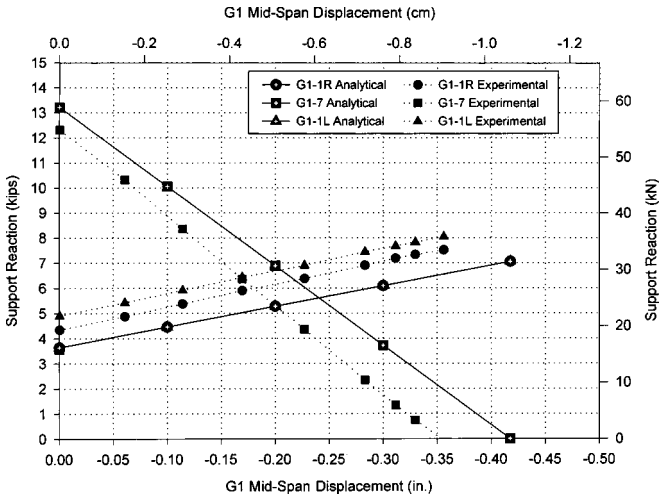

Fig. 8. ES1-4 G1 support reactions versus G1 midspan displacement

simulate the entire structure. Portions of that mesh were used for the erection studies. The erection study simulations were initially run using nominal dimensions and material properties taken from coupon tests. They were later rerun with dimensions taken as averages of measurements obtained from an extensive survey performed during construction and, although minimal improvement (less than 1%) was observed when measured properties were used, those results are presented herein.

Comparisons between analytical and experimental results were completed for five erection study tests: ES1-4, ES1-6, ES2-1, ES2-2, and ES3-1. Loads for the erection study models consisted

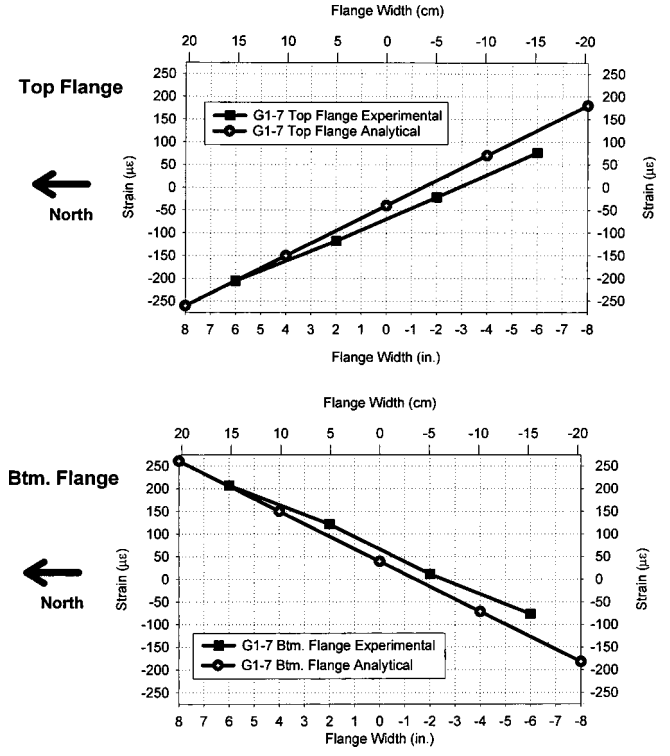

Fig. 9. ES1-4 G1 flange strains, 1.0 cm (0.4 in.) midspan vertical displacement

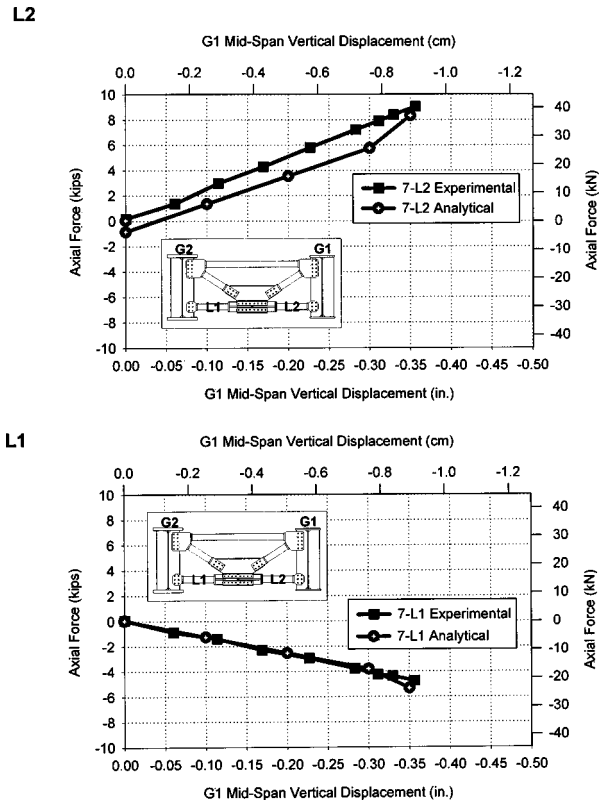

Fig. 10. ES1-4 cross frame 7 lower chord axial forces

of self-weights of the bridge components and additional point loads that accounted for cross-frame connection details not considered in the finite-element models.

Three types of comparisons were made between analytical and experimental results (1) support reactions versus midspan girder displacements; (2) flange and (where applicable) web strain variations for select testing steps; and (3) cross-frame member axial force variations during the "lowering" portion of the erection study tests. Fig. 8 compares support reactions at the abutments (1L and 1R) and at midspan cross frame 7 to midspan displacements for G1 from ES1-4. The shoring frame at cross frame 7 was selected for comparison because that location was typically used

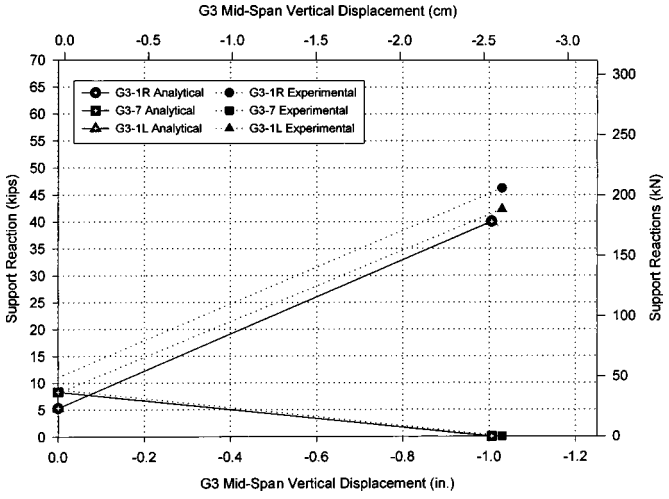

Fig. 11. ES3-1 G3 support reactions versus midspan displacement

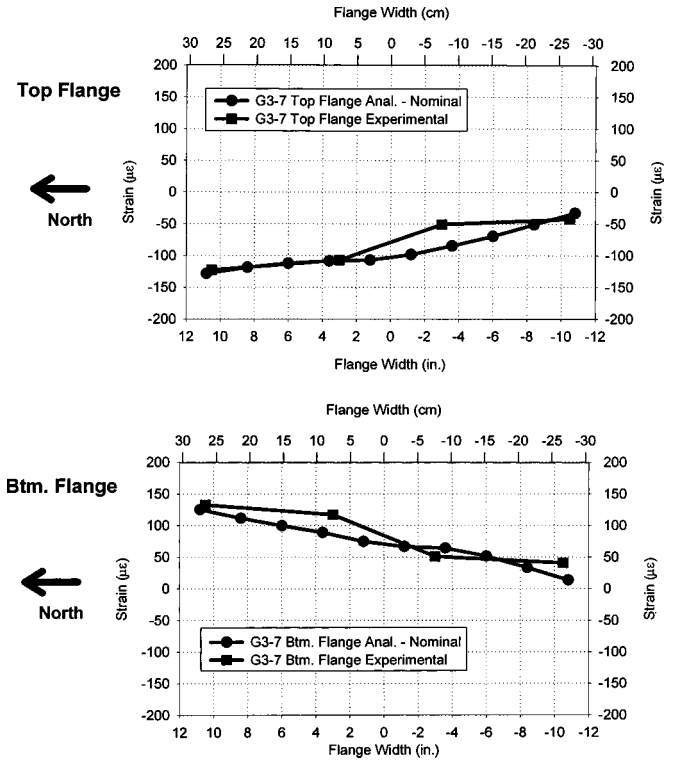

Fig. 12. ES3-1 G3 flange strains, 2.5 cm (1.0 in.) midspan vertical displacement

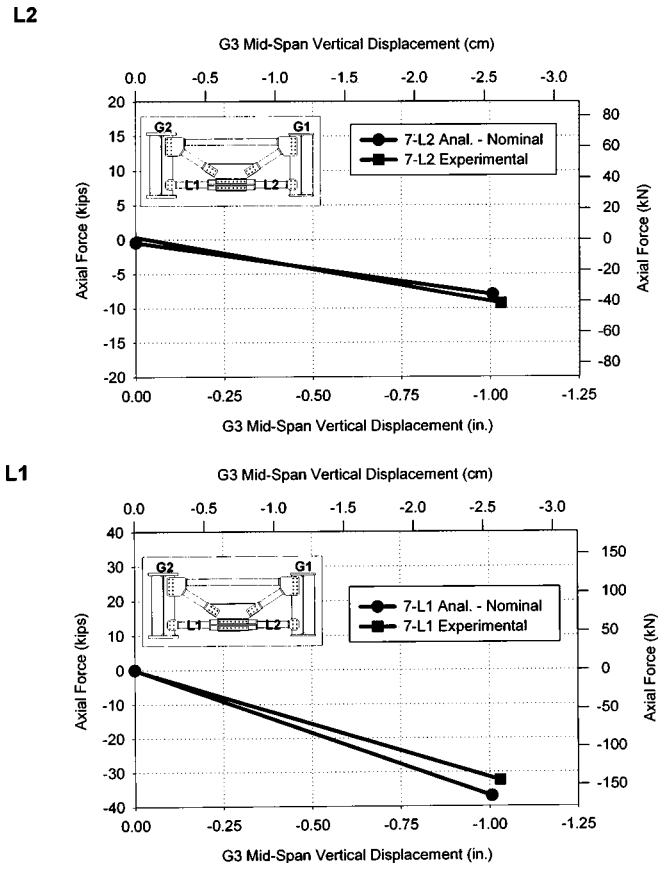

Fig. 13. ES3-1 cross frame 7 lower chord axial forces

to lower girders to their final deformed positions. The figure indicates that the finite-element model predicted the response well, although some discrepancies existed (e.g., symmetry evidenced for 1L and 1R support reactions, maximum 8.0 kN offset for cross frame 7 support reactions, minimum 1 kN offset for 1R reactions). These discrepancies were due to experimental and analytical errors, which consisted of: (1) zero shifts of the data that resulted from heating of instruments and data acquisition system circuitry prior to and during testing; and (2) changes to the structure occurring during fabrication and erection that could not be readily quantified and incorporated into the ABAQUS model. Careful analysis determined that the second explanation was the predominant cause of the discrepancies. After recambering G2, fitting cross frames between the girders required substantial effort and resulted in locked-in forces that could not be measured. Although not shown explicitly in Fig. 8, these studies also indicated that replacing nominal with measured geometric properties had little bearing on the analytical results.

Comparisons between strains across the girder flange at midspan of G1 are shown in Fig. 9 for its maximum deflection during ES1-4. Measured strain values were lower than those estimated analytically, with the maximum difference being 60 $\mu\varepsilon$ at midspan. Two possible causes were identified for these discrepancies. The first was the influence of the cross-frame end connections, which consisted of pairs of large gusset plates at the ends of each tubular member. These gusset plates added stiffness to the as-built structure and additional restraint to the girders and, to reduce solution size, they were not modeled explicitly in ABAQUS. In addition, errors introduced by fabrication and erection tolerances that were not incorporated into the analytical models would have affected the results.

Lower chord axial forces in cross frame 7 that were calculated from measured strains are compared with those predicted from the analytical model in Fig. 10. Comparisons are made throughout the "lowering" portion of test ES1-4. Differences between axial forces obtained from the tests and those predicted from the model approach 9 kN (2 kips), but slopes of the measured and predicted curves are similar, indicating good agreement. Comparative plots for the remaining erection studies indicated similar results to those for ES1-4. Representative results for the final test, ES3-1, are shown in Figs. 11–13. Note that, because ES3-1 incorporated a series of midspan shoring replacement and removal studies, the figures showing the support reaction and cross-frame axial force variations contain data from the first two testing steps. The figures show that the addition of girders and cross frames caused further redistribution of dead loads and, in some cases, an increase in differences between recorded and predicted values. For example, in Fig. 11 the numerical model again predicted a symmetric structure and the maximum difference between predicted and measured reactions approached 31 kN (6 kips). While this difference may appear large, it should be noted that 31 kN (6 kips) constitutes only 5% of the total self-weight of the system for ES3-1.

Table 3 lists experimental and analytical stresses in the G1 flanges for ES1-4. This information was calculated directly from the strains in Fig. 9 assuming linearly elastic behavior. The vast amount of data generated from each erection study test precluded presenting similar tables for ES1-6, ES2-1, ES2-2, and ES3-1. The table indicates that experimental and analytical flange stresses typically differed by 10 MPa (1.5 ksi) or less. While these differences appear large when compared against the absolute (cumulative) flange stresses, they were considered acceptable given assumptions made to obtain certain values (e.g., linearity)

Table 3. ES1-4 G1 Midspan Experimental and Analytical Flange Stresses, 10 mm (0.4 in.) Midspan Vertical Displacement (G1 Girdek)

Flange	Location	Source	Absolute strain ($\mu\varepsilon$)	Absolute stress (MPa)	Vertical bending stress (MPa)	Lateral bending stress (MPa)
Top	Outside (north) tip	Experiment	−250	−50	−16	−34
		Finite-element	−258	−52	−8	−44
	Web	Experiment	−80	−16	−16	0
		Finite-element	−40	−8	−8	0
	Inside (south) tip	Experiment	125	25	−16	41
		Finite-element	178	36	−8	44
Bottom	Outside (north) tip	Experiment	245	49	14	35
		Finite-element	257	51	8	44
	Web	Experiment	70	14	14	0
		Finite-element	39	8	8	0
	Inside (south) tip	Experiment	−120	−24	14	−38
		Finite-element	−178	−36	8	−43

Table 4. G3 Midspan Moment, ES3-1

	Midspan moment [kN-m (k-ft)]			Percent difference	
Girder	Experiment	FEM	V-load	FEM	V-load
G1	41 (30)	39 (29)	−50 (−37)	−3	−220
G3	1,306 (961)	1,395 (1026)	1,333 (980)	7	2

Note: FEM=finite element model.

Table 5. Cross Frame 7 Axial Forces

	ES3-1						
Member	Experiment axial force [kN (kips)]	ABAQUS model axial force [kN(kips)]	Difference from experiment (%)	V-load method axial force [kN (kips)]	Difference from experiment (%)	Cross frame 7 ABAQUS model axial force [kN (kips)]	Difference from experiment (%)
U1	101 (23)	96 (21)	−6	116 (26)	14	102 (23)	1
M1	65 (15)	79 (18)	21	71 (16)	9	77 (17)	18
M2	−54 (−12)	−72 (−16)	32	−71 (−16)	28	−24 (−5)	−56
L1	−144 (−32)	−161 (−36)	12	−174 (−39)	21	−173 (−39)	20
L2	−41 (−9)	−35 (−8)	−16	−96 (−21)	131	−96 (−21)	131

and the low levels of strain/stress experienced by G1 during ES1-4.

V-Load Method

It was of interest to compare results from the V-load method (AISC 1989), an approximate method commonly used by practicioners as a preliminary analysis tool for curved steel bridges, against those from the finite-element models. The name V-load stems from its use of artificial shear forces, labeled "V-loads," applied to the girders at cross-frame connection points. The V-load method replaces actual curved girders with "equivalent" straight girders, which are then analyzed in two steps. First, the "equivalent" straight girders, whose span lengths equal those of the curved girders they represent, are examined under anticipated dead and live loads to determine a series of "primary" moments at each cross-frame connection point. The girders are then reanalyzed under a series of V-loads to determine V-load moments, again applied at the cross-frame connection locations. Resulting primary and V-load moments are superimposed to give the final moments in the curved girder at cross-frame connection points. These moments are then utilized to design the curved girders.

The V-load method was first applied to interior (G1) and exterior (G3) girder midspan moments for ES3-1. The results, shown in Table 4, indicate that both analytical and V-load results estimated experimental G3 midspan moments quite well, with differences being 10% or less. V-load estimations for G1 midspan moment were not nearly as accurate and were nonconservative, with a moment of −50 kN-m (−37 k-ft) being predicted at midspan of G1, while the experimental moment was 41 kN-m (30 k-ft). In contrast to the V-load method, the finite-element model predicted the experimental midspan moment for G1 quite well. Even though the midspan moment magnitudes for G1 were small, the fact that the V-load method gave negative bending at midspan of G1 showed that interior girder moment predictions using this approach could not be considered as accurate as those for the outside girder. These findings match those reported by Fiechtl et al. (1987).

Table 5 compares calculated member forces in cross frame 7 from the finite-element analysis and V-load methods to values from experimental data for ES3-1. The V-load method provided forces that were conservative when compared with experimental results. One of the predicted axial forces, that for member L2, was more than double that found experimentally. These differences were attributed to assuming that the cross frame behaved as

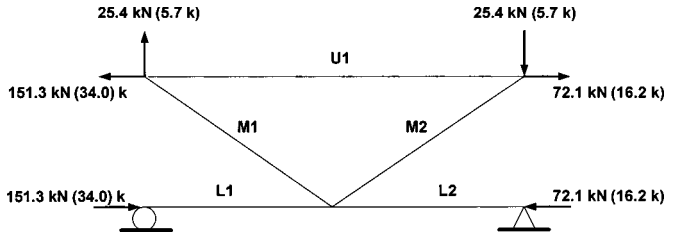

Fig. 14. Cross frame 7 two-dimensional finite-element model

a truss. To investigate whether analyzing cross frame 7 as a frame would produce more accurate predictions, a simple two-dimensional frame model of a representative cross frame was prepared and analyzed, using ABAQUS PIPE21 elements to represent the tubular members. Loads determined using V-load criteria were applied to the cross frame as shown in Fig. 14. To prevent rigid body motion, restraints were provided at lower member ends as shown in the figure. Results from this analysis are also listed in Table 5, and they do not indicate beneficial improvement over results obtained assuming truss behavior with the V-load method.

Conclusions

A series of erection study tests were conducted to shed light on the capability of analytical tools for predicting response during erection. The tests demonstrated the beneficial effects of providing minimal radial restraint for curved I-girders during construction and also the effects of nonuniform shoring removal on response.

Comparisons between experimental data and results from finite-element analyses showed good predictions of erection behavior. Discrepancies between the predicted and measured support reactions, deformations, and member forces that arose were mainly attributed to fabrication and erection sequence effects changing load distribution patterns in the experimental structures. While it was apparent that the fabrication and erection techniques has an impact on behavior, a detailed study of their effects could not be completed, as uncertainties associated with the magnitudes of forces and deformations that were "locked into" the experimental bridge during fabrication and construction could not be accurately quantified and incorporated into the analytical models.

It was shown that replacing nominal geometric and material properties with measured properties in the finite-element model did not significantly improve analytical results. In addition, it appears that simplifying analytical representations of cross-frame connection details in a finite-element model may provide inaccurate representations of radial load distributions in a curved steel girder bridge system.

When forces were estimated using the V-load method, it was shown that conservative predictions of outside girder (G3) moments and nonconservative predictions of moments in the inside girder (G1) were provided. The V-load method also provided conservative predictions of cross-frame axial forces. While these results match previous findings, it should be noted that they were obtained for a unique simply supported curved bridge system and that different findings may exist for more complicated systems containing additional girders and continuous spans.

Acknowledgments

This work is supported by HDR Engineering through FHWA Contract No. DTFH61-92-C-00136. Sheila Duwadi served as the Contracting Officer's Technical Representative for FHWA. The technical input of Dann Hall and Mike Grubb of BSDI and John Yadlosky of HDR was invaluable to this investigation. The tests were carried out at the FHWA Turner-Fairbank Laboratory in McLean, VA, and the assistance of Bill Wright, Joseph Hartmann, and the rest of the FHWA staff is gratefully acknowledged. The contributions of James Burrell of Qualcomm, Inc., who generated the original finite-element model, are also gratefully acknowledged.

References

American Association of State Highway and Transportation Officials (AASHTO). (1980). *Guide specifications for horizontally curved bridges*, Washington, D.C.

American Association of State Highway and Transportation Officials (AASHTO). (1993). *Guide specifications for horizontally curved bridges*, Washington, D.C.

American Association of State Highway and Transportation Officials (AASHTO). (2003). *Guide specifications for horizontally curved bridges*, Washington, D.C.

American Institute of Steel Construction (AISC) Marketing, Inc. (1989). *AASHTO curved-girder bridge design specifications, AISI Transportation Structure Subcommittee*, Chicago.

Armstrong, W. L. (1972). "Dynamic testing of curved bridge-Huyck stream." *ASCE J. Struct. Div.*, 98(9), 2015–2030.

Brennan, P. J. (1970). "Horizontally curved bridges first annual report: analysis of horizontally curved bridges through three-dimensional mathematical model and small scale structural testing." *First Annual Rep., Research Project HPR-2(111)*, Syracuse University, Syracuse, N.Y.

Brennan, P. J. (1971). "Horizontally curved bridges second annual report: analysis of Seekonk River Bridge small scale structure through three-dimensional mathematical model and small scale structural testing." *Second Annual Rep., Research Project HPR-2(111)*, Syracuse University, Syracuse, N.Y.

Colville, J. (1973). "Tests of curved steel-concrete composite beams." *ASCE J. Struct. Div.*, 99(7), 1555–1570.

Fiechtl, A. L., Fenves, G. L., and Frank, K. H. (1987). "Approximate analysis of horizontally curved girder bridges." *Final Rep. No. FHWA-TX-91-360-2F*, Center for Transportation Research, Texas Univ., Austin, Austin, Tex.

Galambos, T. V., Hajjar, J. F., Leon, R. T., Huang, W., Pulver, B. E., and Rudie, B. J. (1996). "Stresses in steel curved girder bridges." *Rep. No. MN/RC-96/28*, Minnesota Dept. of Transportation, St. Paul, Minn.

Hall, D. H., Grubb, M. A., and Yoo, C. H. (1999). "Improved design specifications for horizontally curved steel girder highway bridges." *Research Rep. 424*, National Cooperative Highway Research Program, Washington, D.C.

Hanshin Expressway Public Corporation. (1988). *Guidelines for the design of horizontally curved girder bridges (draft)*, Osaka, Japan.

Huang, W. H. (1996). "Curved I-girder systems." PhD thesis, Dept. of Civil Engineering, Univ. of Minnesota, Minn.

Kitada, T., Nakai, H., and Murayama, Y. (1993). "State-of-the-art on research, design, and construction of horizontally curved bridges in Japan." *Proc., Annual Technical Session*, Structural Stability Research Council, Rolla, Mo.

Linzell, D. G. (1999). "Studies of a full-scale horizontally curved steel I-girder bridge system under self-weight." PhD thesis, School of Civil and Environmental Engineering, Georgia Institute of Technology, Atlanta.

Mozer, J., Cook, J., and Culver, C. (1973). "Horizontally curved highway

bridges–stability of curved plate girders." *Rep. No. P3, Research Project HPR–2(111)*, Carnegie Mellon University, Pittsburgh.
Mozer, J., and Culver, C., (1970). "Horizontally curved highway bridges–stability of curved plate girders." *Rep. No. P1, Research Project HPR–2(111)*, Carnegie Mellon University, Pittsburgh.
Mozer, J., Ohlson, R., and Culver, C. (1971). "Horizontally curved highway bridges–stability of curved plate girders." *Rep. No. P2, Research Project HPR–2(111)*, Carnegie Mellon University, Pittsburgh.
Shanmugam, N. E., Thevendran, J. Y., Liew, R., and Tan, L. O. (1995). "Experimental study on steel beams curved in plan." *J. Struct. Eng.*, 121(2), 249–259.
Thevendran, J. Y., Shanmugam, N. E., and Liew, R. (1998). "Flexural torsional behavior of steel I-beams curved in plan." *J. Constr. Steel Res.*, 46(1–3), 79–80.
Yadlosky, J. M. (1991). "Horizontally curved steel girders: Questions and concerns." *Proc., 8th Annual Int. Bridge Conf.*, 266.
Yoo, C. H., and Carbine, R. L. (1985). "Experimental investigation of horizontally curved steel wide flange beams analysis." *Proc., Annual Technical Session: Stability Aspects of Industrial Buildings*, Structural Stability Research Council, Rolla, Mo., 183–191.
Zureick, A., and Naqib, R. (1999). "Horizontally curved steel I-girders state-of-the-art analysis methods." *J. Bridge Eng.*, 4(1), 38–47.
Zureick, A., Naqib, R., and Yadlosky, J. M. (1994). "Curved steel bridge research project. Interim report I: Synthesis." *Rep. No. FHWA-RD-93-129*, HDR Engineering, Inc., Omaha, Neb.